Hindawi
International Journal of Antennas and Propagation
Volume 2019, Article ID 8183153, 9 pages
https://doi.org/10.1155/2019/8183153

Research Article

A Horizontal Azimuth Pattern-Reconfigurable Antenna Using Omnidirectional Microstrip Arrays for WLAN Application

Liang Yang[1], **Cheng Lu**[1], **Xiao Li**[1], **Leilei Liu**[2] **and Xiaoxing Yin**[1]

[1]*State Key Laboratory of Millimeter Waves, Southeast University, Nanjing 210096, China*
[2]*Nanjing University of Posts and Telecommunications, Nanjing 210003, China*

Correspondence should be addressed to Xiaoxing Yin; 101010074@seu.edu.cn

Received 21 August 2018; Revised 23 November 2018; Accepted 4 December 2018; Published 25 February 2019

Academic Editor: Farid Ghanem

A horizontal azimuth pattern-reconfigurable antenna with configurable parasitic element arrays for WLAN applications is proposed in this paper. It consists of a control board, a central series-fed omnidirectional microstrip array, four configurable parasitic elements, a bottom conducting plate, and a top supporting plate. The omnidirectional microstrip array is adopted as an exciter, around which the four same parasitic element arrays are arranged at four corners. The p-i-n diodes as switches are placed between the parasitic element arrays and the conducting plate to control the fifteen radiation patterns of the proposed antenna. The parasitic element arrays are configured as reflectors or directors by switching the p-i-n diodes on or off. The bandwidth achieved ranges from 5.00 GHz to 5.27 GHz. A gain of 8.52 dBi is obtained when the antenna reaches the maximum gain in the H-plane at 5.2 GHz. Good agreements between the simulated and measured results were observed. The proposed parasitic structure which has the same structure with the driven element can enhance the horizontal azimuth gain of the antenna. Only 4 p-i-n diodes are used to produce up to 15 useful beam configurations with a gain range of 4.56-8.52 dBi at the horizontal azimuth.

1. Introduction

With the development of the wireless communication, multifunctional and reconfigurable antennas are widely used [1–3] and become more desired. The pattern reconfiguration of the antennas is of significance in the telecommunication. Thus, smart pattern-reconfigurable antennas are expected strongly [4–8].

Antennas used in the wireless communication usually have omnidirectional radiation patterns, so as to cover all horizontal azimuth. Consequently, the horizontal azimuth patterns in WLAN and wireless communication applications have attracted more attention. However, customers are not uniformly distributed, and the numbers of terminals always change in different directions at the antenna horizontal azimuth. The constant omnidirectional pattern at all working time leads to a waste of radiation power. Many reconfigurable antenna solutions have been studied [9–20]. Literature [9] proposed the H-shaped resonator structure controlled by the p-i-n diodes to reconfigure the pattern of the driven element. It is able to switch between the broadside pattern and the end-fire pattern. Nevertheless, the limited three states and unstable feed board connected with the antenna board constrict its application. In [10], a circle planar reconfigurable antenna with various patterns is developed, achieving two operating frequencies and 6 beam directions, totally 12 operating modes is ready. Literature [11] puts forward a reconfigurable antenna array for some handheld terminals and MIMO applications, achieving a high gain. The antenna design in [12–15] has the horizontal azimuth-pattern-reconfigurable ability but limited states for the complex applications. Literature [16–19] develop a planar structure antenna with 9 states, not strictly in a horizontal azimuth pattern reconfigurable mode. Most of the beams steer in the vertical direction of the antenna plane. In [20], the antenna with a planar structure has eight stable beams covering all the directions at an azimuth plane of $\theta = 36^{\circ}$. These antennas are more suitable for top ceiling antenna applications.

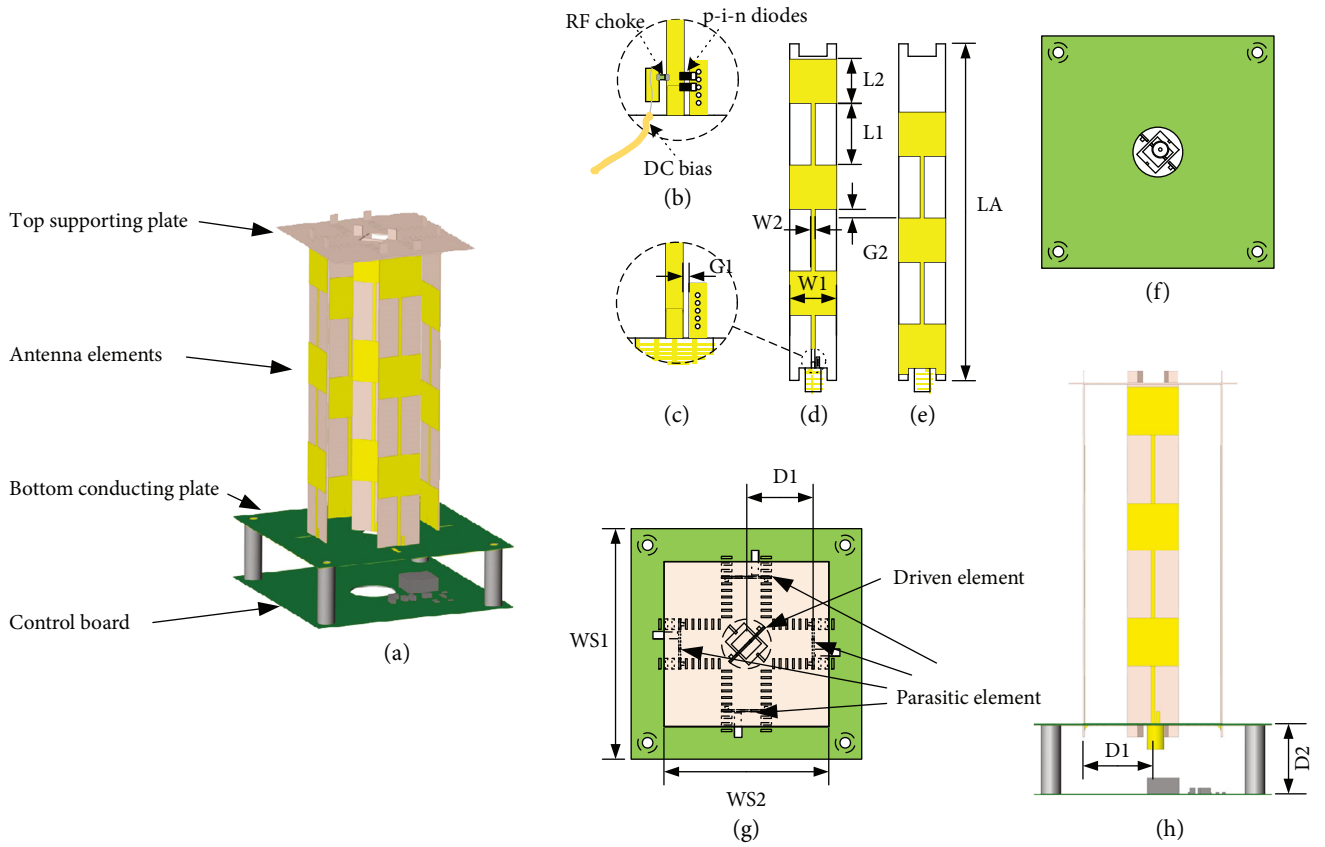

Figure 1: The details of the proposed antenna structure. (a) The structure of the proposed antenna. (b) The partial view of parasitic element arrays bias circuit with p-i-n diodes. (c) The partial view of the exciter probe circuit. (d) The top view of exciter. (e) The bottom view of exciter. (f) The bottom view of the proposed antenna. (g) The top view of the proposed antenna. (h) The side view of the proposed antenna. The dimension of the antenna is as follows: LA = 108 mm, L1 = 20 mm, L2 = 14 mm, W1 = 15 mm, W2 = 1.1 mm, G1 = 0.4 mm, G2 = 3 mm, WS1 = 70 mm, WS2 = 50 mm, D1 = 20 mm, and D2 = 20 mm.

This paper presents a horizontal azimuth pattern-reconfigurable omnidirectional microstrip array antenna with parasitic element arrays. An omnidirectional microstrip array antenna [21, 22] is adopted as an exciter, around which the four uniform parasitic element arrays are arranged at four corners. The same structure of the parasitic element arrays and the driver antenna keeps the maximum gain at the horizontal azimuth. The p-i-n diodes as switches are placed between parasitic element and conducting plate to control the fifteen radiation patterns. The parasitic element arrays can be configured as reflectors or directors through switching of the p-i-n diodes. The proposed reconfigurable antenna with diverse patterns is able to satisfy different WLAN applications. The following sections will present a prototype antenna fabricated, and the description of measured results and all of the pattern states will be given.

2. Antenna Structure and Design

An antenna that truly enables horizontal azimuth pattern reconfiguration is committed to be provided. The antenna is designed 4 reconfigurable parasitic elements and a driven element. The reconfigurable parasitic elements, which can be configured as directors and reflectors, are controlled by the p-i-n switches. The proposed antenna, shown in Figure 1(a), consists of a control board, series-fed omnidirectional microstrip array antenna at the center of the proposed antenna, four configurable parasitic element arrays, a bottom conducting plate, and a supporting top plate.

2.1. The Driven Antenna Design. The series-fed omnidirectional microstrip array antenna acts as an exciter [22], with detailed dimension shown in Figure 1(c), (d), and (e). The microstrip antenna array has six radiation elements in series, among which are on one face of the substrate connected to the inner conductor of feeding SMA connector; the rest are on the other face of the substrate connected to the exterior conductor of the feeding SMA connector. The lengths of each microstrip-fed line and the radiation element are, respectively, approximately a half wavelength at the central operating frequency. This keeps the current on each wide radiation elements almost in phase, thereby combining in the horizontal azimuth direction and producing an omnidirectional pattern [22]. The current and the electric field distribution of the central driven element is demonstrated in Figures 2(a) and 2(b). The simulated pattern of the driven element at 5.2 GHz is shown in Figure 2(c).

2.2. The Parasitic Element Design and Configuration. The parasitic element arrays surrounding the exciter have the

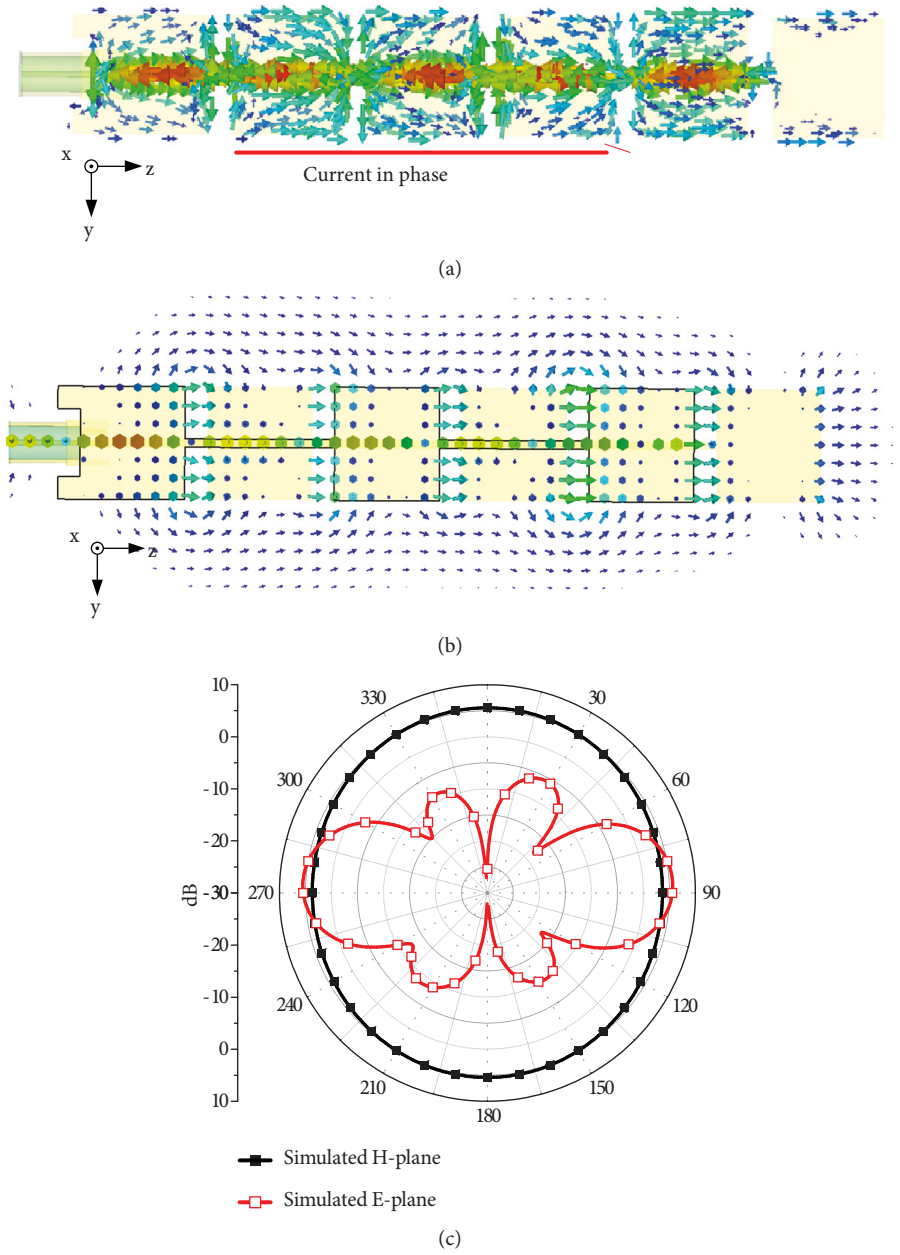

Figure 2: (a) The current distribution of the driven element of the proposed antenna structure. (b) The electric field distribution of the driven element of the proposed antenna structure. (c) The simulated pattern of the driven element at 5.2 GHz.

same structure and dimensions as the exciter. The inside faces of the parasitic arrays are towards the exciter, and the outside faces are backwards the exciter. Three radiation elements are on the inside face, among which the one close to the conducting plate is connected to the conducting plate. The rest radiation elements are on the outside face, among which the element close to the conducting plate is connected to the anode of a p-i-n diode. In this way, the cathode of the p-i-n diode is connected to the radiation element on inside face and then to the conducting plate. The square conducting plate and top supporting plate of the antenna are fabricated with RO4003C substrate. Both the plates have slots to hold and fix the exciter and the parasitic element arrays on them, as shown in Figure 1(g). The Infineon p-i-n diode of BAR50-02V is embedded in the proposed antenna. An SC-79-2 package of the p-i-n diode is selected to fit the gap between two conductors at the bias circuit of the parasitic element arrays. In practice, the driven current is set at 100 mA, so that the p-i-n diode achieves the minimum insertion loss. In addition, Murata inductors of LQG15HN2N7C02D (2.7 nH) are mounted at the bias circuit in the path of the p-i-n diodes as RF chokes. The isolation of the p-i-n diode is 12.5 dB, and the insertion loss is 0.17 dB at 5 GHz. To achieve a good isolation, two p-i-n diodes are mounted in parallel at the gap between the two conductors. The partial view of parasitic element arrays bias circuit is presented in

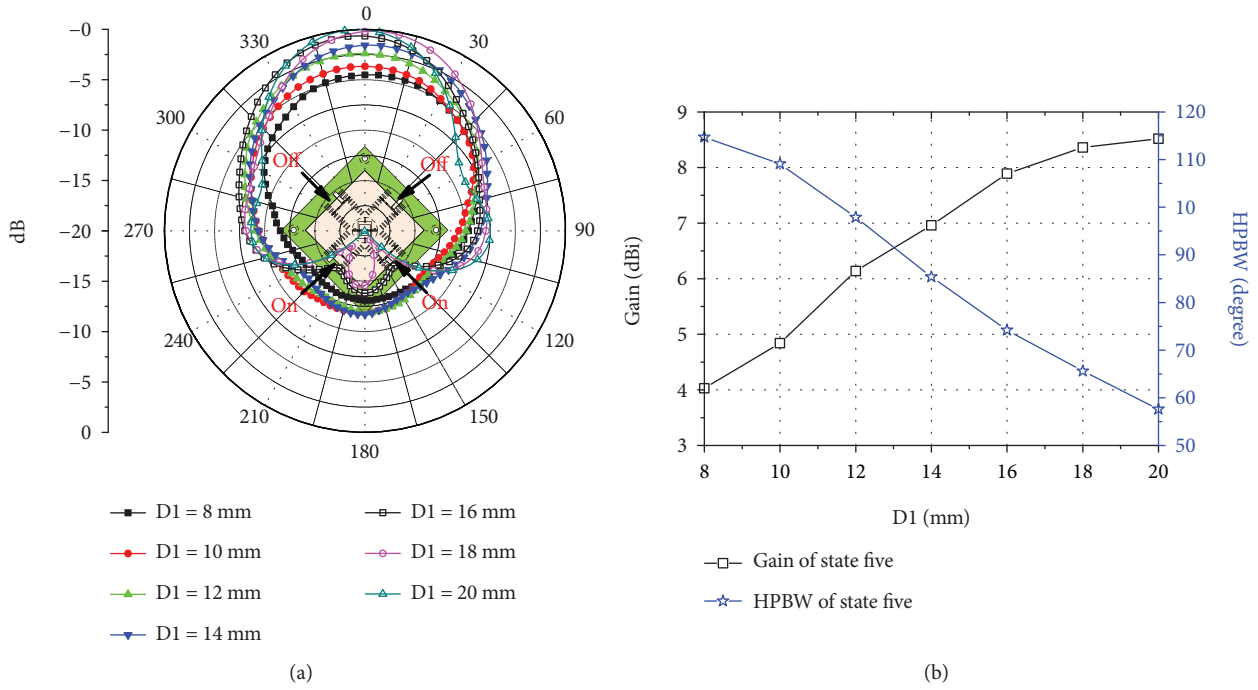

Figure 3: (a) Patterns of different distance state V with different distance of D1 measured at 5.2 GHz. (b) Gain and HPBW of state V with different distance of D1 measured at 5.2 GHz.

Figure 1(b). The radiation patterns of the proposed antenna at the state V with different distance D1 are measured, with the results shown in Figure 3. This step helps to investigate the effect of the distance D1 between parasitic element arrays at the corner and the exciter. The rise of D1 leads to an increase in the gain but decrease in the HPBW. For a higher gain, the distance D1 is optimized to 20 mm, which is 0.35 λ_0 wavelength. It is wider than the size of Yagi antenna's parasitic elements with driven element.

2.3. The States of p-i-n Diodes Configurations. The states of p-i-n diodes determine the property of the parasitic element arrays. The p-i-n diodes are turned on when their DC bias on a parasitic element array are high. In this case, the parasitic element arrays act as reflectors, and the main beam of the proposed antenna is switched to the direction from the parasitic element array to the exciter on a horizontal plane. When the p-i-n diodes on a parasitic element array are turned off, the radiation elements on the outside face are disconnected to the conducting plate. Then, the parasitic element arrays act as directors, and the main beam of the exciter is enhanced in the directions from the exciter to the parasitic element arrays. The proposed antenna includes four groups of p-i-n diodes in four corners, each of which has two states. Thus, the proposed total of 16 pattern configurations are obtained.

The 16 pattern configurations can be categorized into 6 states as follows. At state I and II, all of the p-i-n diodes are turned on and off, respectively. At state III, one group of the p-i-n diodes is turned on and the others are turned off, contrary to state IV. At state V, two groups of adjacent p-i-n diodes are turned on. At state VI, two groups of p-i-n diodes at opposite position are turned on. There are four radiation patterns, respectively, from state III to state V, but 2 patterns at state VI. The 16 pattern configurations with the 04 states of the p-i-n diodes are listed in Table 1. The state *OA is the single driven element without parasitic elements.

Table 1: Different configuration states of the proposed antenna.

State	p-i-n1	p-i-n2	p-i-n3	p-i-n4	Gain (dBi)	HPBW (°)
*OA					3.91	
I	On	On	On	On	-1.64	88.200
II	Off	Off	Off	Off	5.09	243.50
III	On	Off	Off	Off	6.01	299.90
	Off	On	Off	Off	5.99	275.70
	Off	Off	On	Off	5.71	277.90
	Off	Off	Off	On	5.93	283.70
IV	Off	On	On	On	5.96	108.70
	On	Off	On	On	5.53	111.80
	On	On	Off	On	5.56	115.70
	On	On	On	Off	5.94	106.90
V	On	On	Off	Off	8.52	57.00
	Off	On	On	Off	7.62	80.10
	Off	Off	On	On	8.10	70.00
	On	Off	Off	On	7.35	81.20
VI	Off	On	Off	On	5.43	81.30
	On	Off	On	Off	4.56	79.30

* OA: the original antenna without parasitic elements.

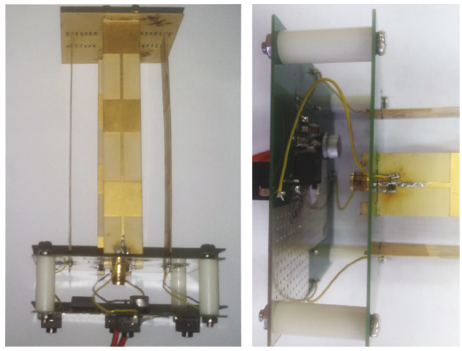

Figure 4: The photograph of the fabrication of the proposed antenna.

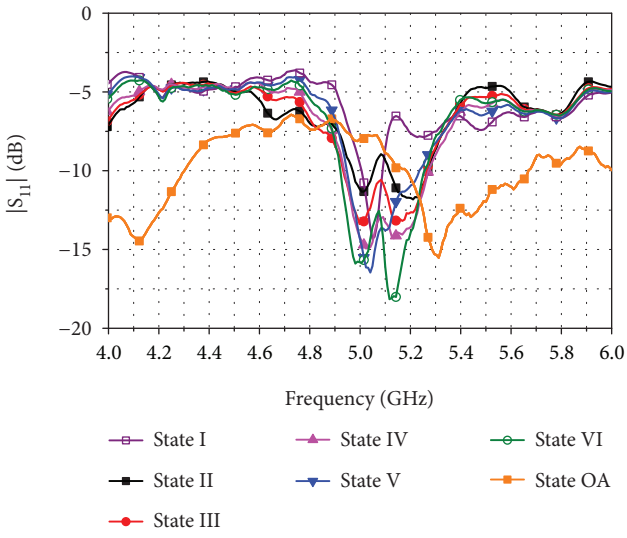

Figure 5: Reflection coefficients of omnidirectional microstrip antenna with the different states of the p-i-n diodes and the original omnidirectional microstrip antenna.

3. Simulation and Measurement Results

A prototype of the proposed antenna is fabricated and assembled, as shown in Figure 4. The exciter and the parasitic element arrays are fabricated by two-layer PCBs using a substrate of Rogers RO4003C with 3.55 of dielectric constant, 0.0027 of loss tangential, and 0.508 mm of thickness. The top supporting plate is also fabricated by the Rogers RO4003C substrate with the same thickness but nonmetalized for reducing the impact on the antenna array. The bottom conducting plate and the control plate are fabricated by thick FR4 substrates with thickness of 1 mm to obtain mechanical stability. The distance between the two plates is 20 mm. The bottom FR4 conducting substrate is metalized to eliminate impacts of noise and radiation on power supply and control circuits.

The reflection coefficients of the proposed antenna with different states and the original antenna are measured by the vector network analyzer Keysight E5071C, with results shown in Figure 5. It can be seen from the comparison that the reflection coefficients with and without the parasitic elements are significantly different due to the strong mutual coupling between the driven antenna and the parasitic elements. Due to the mutual coupling effect, the operating frequency is reduced from 5.3 GHz to 5.1 GHz, which is also our target operating frequency band. Except for state I and II, the central operating frequency band of the proposed antenna is 4.94 GHz-5.27 GHz, with a 6.46% bandwidth under -10 dB of the reflection coefficient. The p-i-n diodes of the state I and II are all on or all off. The two states are special omnidirectional patterns, having different radiation resistor for the driven element. All the reflection coefficients of directional patterns for the proposed antenna with parasitic element arrays of 4 p-i-n diode states are compared. It is demonstrated that the parasitic element arrays loading the four states of p-i-n diodes have negligible impacts on reflection coefficients, which is important for a practical reconfigurable antenna array. On the other hand, these arrays impose a negligible effect on the input port of the proposed antenna, which is a key factor to develop this type of reconfigurable antenna.

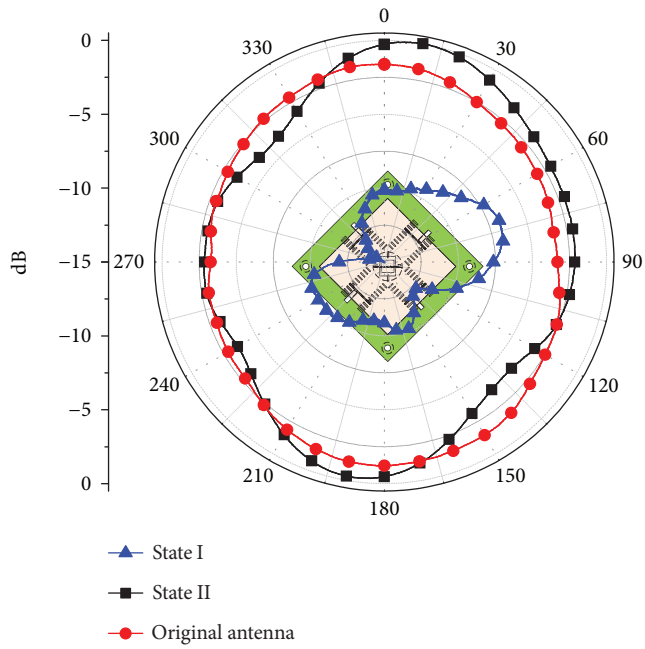

Figure 6: The H-plane pattern of state I (blue trace), state II (black trace), and the original antenna (red trace) at 5.2 GHz.

The 16 far-field radiation patterns, as well as the radiation pattern of the original omnidirectional microstrip array antenna without parasitic element arrays, are measured. The H-plane radiation patterns of the proposed antenna at states I and II, as well as the original antenna without parasitic element arrays, are shown in Figure 6. The measured results indicate that directors enhance the gain in the direction from the exciter to directors. In state II, because all of the four parasitic element arrays worked as directors, 4 main lobes with directions towards the diagonal gaps of adjacent parasitic element arrays are obtained. When the proposed antenna works at state I,

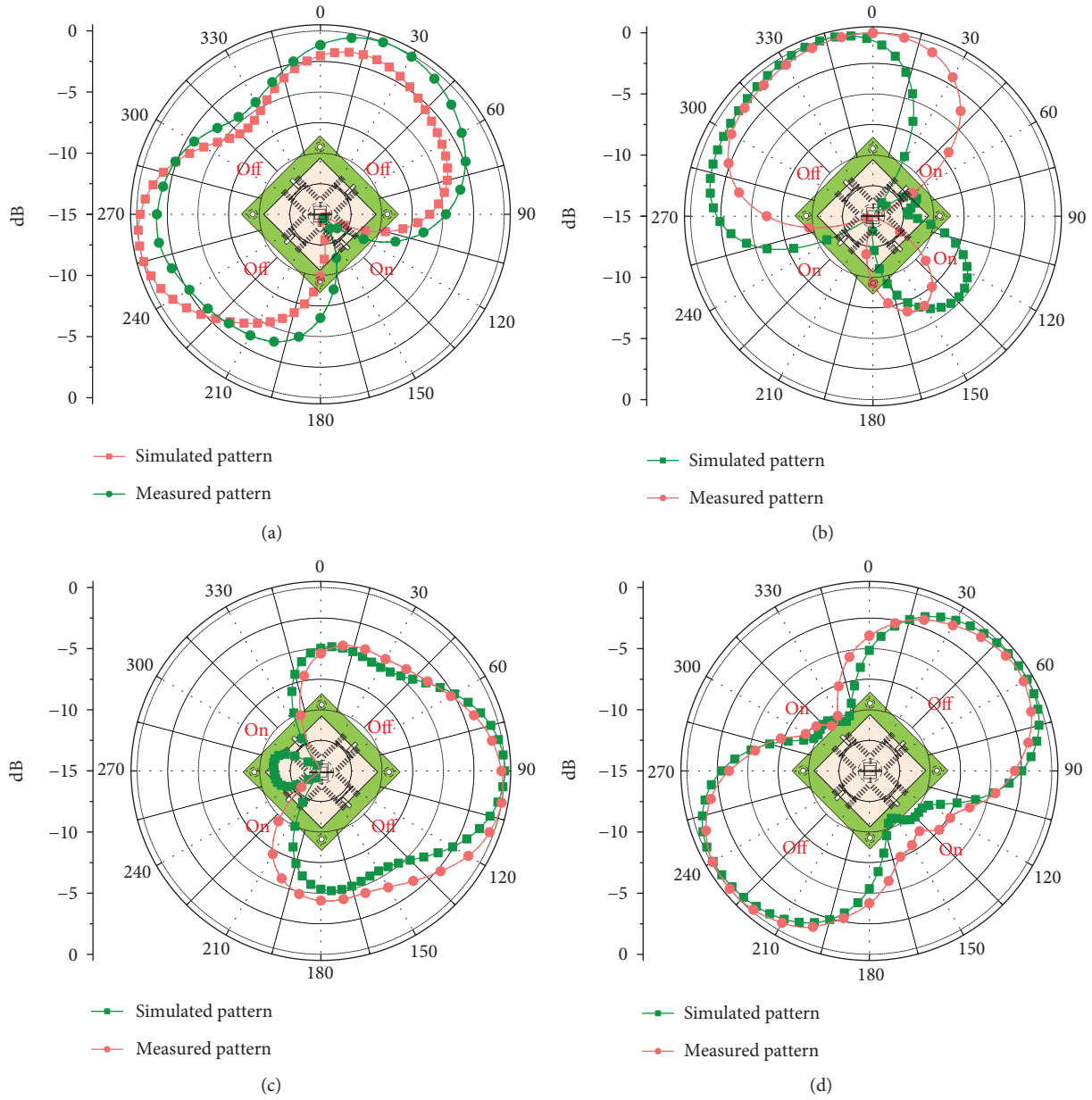

Figure 7: The simulated and measured normalized H plane patterns of states III (a), IV (b), V (c), and VI (d) of the proposed antenna at 5.2 GHz, and the p-i-n modes indicated on the figure.

the parasitic element arrays act as reflectors, then the radiation of the exciter gets rejected in four corner directions. Thus, state I can be regarded as an illegal state of the proposed antenna on the horizontal plane. The normalized radiation pattern of other directional pattern states in simulation and measurement is shown in Figure 7. Each pattern of the directional states with four beams is illustrated in Figure 8, respectively. The proposed antenna at state III has a gain of 5.99 dBi and a wide HPBW, as shown in Figure 8(a). The radiation pattern at state III is applicable to the situations where the signal at a certain direction of the radiation pattern needs to be canceled. As shown in Figure 8(b), the proposed antenna at state IV has a gain of 5.94 dBi lower than that at state III but also a narrower HPBW and a higher quality pattern. The radiation pattern at state V, as shown in Figure 8(c), covers a wide horizontal azimuth angle but not omnidirectional and has a high directional gain of 8.52 dBi. This pattern is suitable for the situations where users of Wi-Fi are in a crowded area at a very narrow horizontal azimuth angel. This is because improving the gain of the antenna in the certain direction contributes to a higher communication quality. The radiation pattern of state VI is specifical, as shown in Figure 8(d). It is applicable when the customers are at the two sides opposite of the antenna. At last, the 15 useful beams have obtained with 5 p-i-n configurable state. The detailed measurement gains and HPBW of each beams are listed in Table 1. The simulated radiation efficiency of the proposed antenna is over 78%.

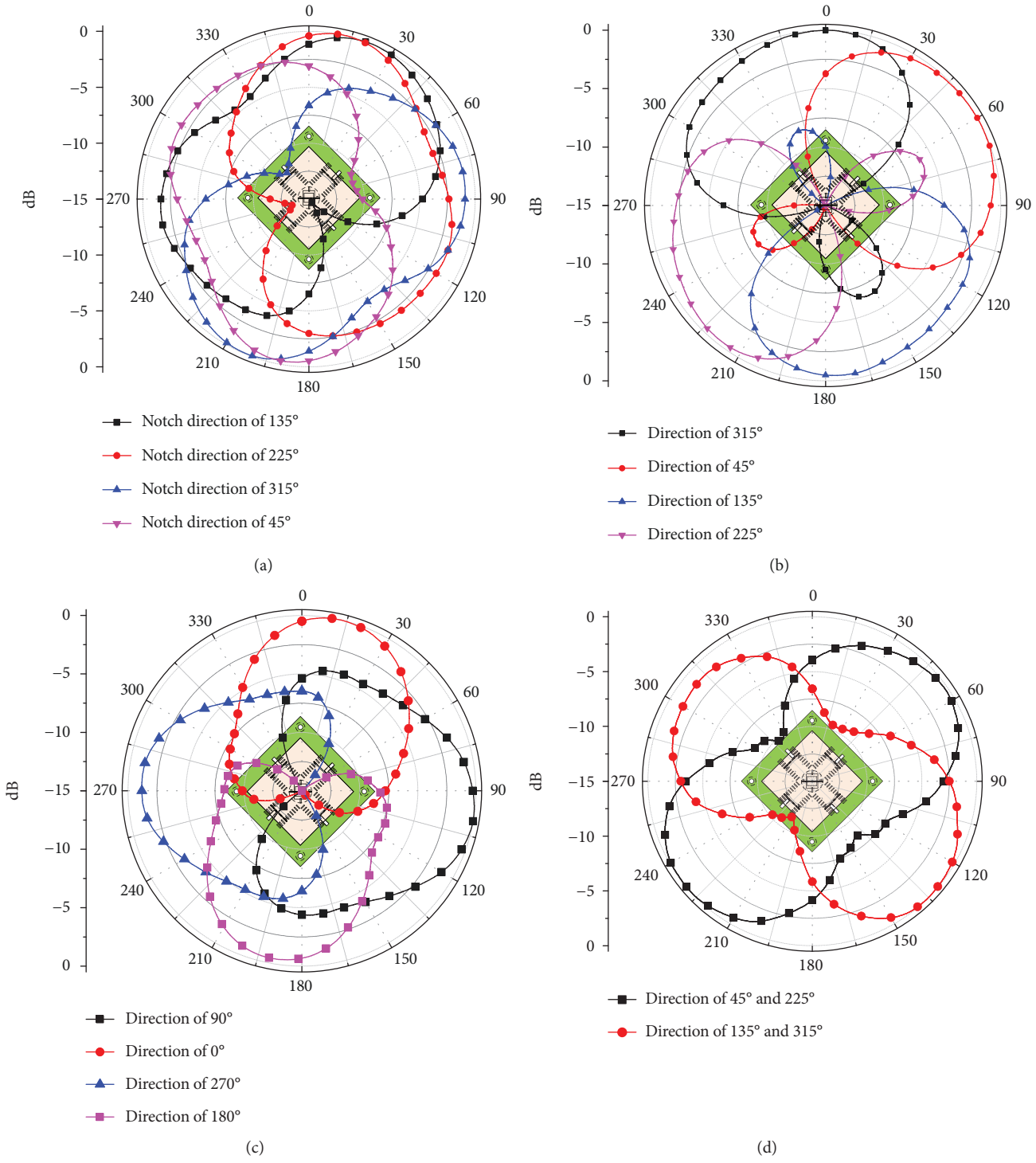

FIGURE 8: Measured patterns of the four states at 5.2 GHz, (a) state III, a reflector and three directors, (b) state IV, three reflectors and a director, and (c) state V, two reflectors and two directors, which are adjacent (d) state VI, two reflectors and two directors, which are not adjacent.

Compared with the reference paper, shown in Table 2, the proposed antenna has both a large structure and diversified patterns in horizontal azimuth direction at the single operating band. It can be embedded into the home media center of the proposed antenna, thereby adapting the customer's distribution to more complex applications.

4. Conclusion

This paper proposes a horizontal azimuth pattern-reconfigurable antenna using omnidirectional microstrip array loaded with configurable parasitic elements. Driven by four p-i-n diodes, the proposed antenna can produce 15

Table 2: Comparison of proposed and reference antennas.

Paper	Center freq. (GHz)	Gain (dBi)	State amount	Beams	Total size (λ_0)
8	2.47–2.9	6.4	3	3	Planar: 0.716*0.537
9	2.28–2.58 & 2.62–2.73	4.3 & 3.6	2	12	Planar: radius = 0.405
10	5	9.7–11	3	3	3D:2.41*0.15*0.01
11	5.35–6.45	4.67–6.09	2	4	Planar: 1.38*1.38
16	2.38	7	3	9	Planar: 0.952*0.952
19	2.35–2.61	4.5	1	8	Planar:
This work	5.2	5.09–8.52	5	15	3D:1.93*1.21*1.21

radiation patterns, thus satisfying diverse requirements of WLAN application. The measured results of the prototype are well in line with the simulated ones. The simple structure facilitates its implementation in certain low-cost devices not only WLAN but also many other wireless communications.

Data Availability

The simulation and measurement data used to support the findings of this study are included within the paper. The structures are simulated and analyzed by CST microwave studio.

Conflicts of Interest

The authors declare that they have no conflicts of interest.

Acknowledgments

This work was supported in part by the National Natural Science Foundation of China under Grants 61427801, 61771127, U1536123, and U1536124.

References

[1] N. Haider, D. Caratelli, and A. G. Yarovoy, "Recent developments in reconfigurable and multiband antenna technology," *International Journal of Antennas and Propagation*, vol. 2013, Article ID 869170, 14 pages, 2013.

[2] W. Wu, B. Z. Wang, X. S. Yang, and Y. Zhang, "A pattern-reconfigurable planar fractal antenna and its characteristic-mode analysis," *IEEE Antennas and Propagation Magazine*, vol. 49, no. 3, pp. 68–75, 2007.

[3] R. L. Haupt and M. Lanagan, "Reconfigurable antennas," *IEEE Antennas and Propagation Magazine*, vol. 55, no. 1, pp. 49–61, 2013.

[4] R. Vaughan, "Switched parasitic elements for antenna diversity," *IEEE Transactions on Antennas and Propagation*, vol. 47, no. 2, pp. 399–405, 1999.

[5] H. L. Zhu, S. W. Cheung, and T. I. Yuk, "Mechanically pattern reconfigurable antenna using metasurface," *IET Microwaves, Antennas & Propagation*, vol. 9, no. 12, pp. 1331–1336, 2015.

[6] W. Q. Deng, X. S. Yang, C. S. Shen, J. Zhao, and B. Z. Wang, "A dual-polarized pattern reconfigurable Yagi patch antenna for microbase stations," *IEEE Transactions on Antennas and Propagation*, vol. 65, no. 10, pp. 5095–5102, 2017.

[7] J. Li, Q. Zeng, R. Liu, and T. A. Denidni, "A compact dual-band beam-sweeping antenna based on active frequency selective surfaces," *IEEE Transactions on Antennas and Propagation*, vol. 65, no. 4, pp. 1542–1549, 2017.

[8] L. Han, C. Wang, W. Zhang, R. Ma, and Q. Zeng, "Design of frequency- and pattern-reconfigurable wideband slot antenna," *International Journal of Antennas and Propagation*, vol. 2018, Article ID 3678018, 7 pages, 2018.

[9] J. Ren, X. Yang, J. Yin, and Y. Yin, "A novel antenna with reconfigurable patterns using H-shaped structures," *IEEE Antennas and Wireless Propagation Letters*, vol. 14, pp. 915–918, 2015.

[10] T. Guo, W. Leng, A. Wang, J. Li, and Q. Zhang, "A novel planar parasitic array antenna with frequency- and pattern-reconfigurable characteristics," *IEEE Antennas and Wireless Propagation Letters*, vol. 13, pp. 1569–1572, 2014.

[11] N. H. Chamok, M. H. Yılmaz, H. Arslan, and M. Ali, "High--gain pattern reconfigurable MIMO antenna array for wireless handheld terminals," *IEEE Transactions on Antennas and Propagation*, vol. 64, no. 10, pp. 4306–4315, 2016.

[12] Y. F. Cheng, X. Ding, B. Z. Wang, and W. Shao, "An azimuth-pattern-reconfigurable antenna with enhanced gain and front-to-back ratio," *IEEE Antennas and Wireless Propagation Letters*, vol. 16, pp. 2303–2306, 2017.

[13] T. Zhang, S. Y. Yao, and Y. Wang, "Design of radiation-pattern-reconfigurable antenna with four beams," *IEEE Antennas and Wireless Propagation Letters*, vol. 14, pp. 183–186, 2015.

[14] I. Ben Trad, J. M. Floc'h, H. Rmili, M.'. Drissi, and F. Choubani, "A planar reconfigurable radiation pattern dipole antenna with reflectors and directors for wireless communication applications," *International Journal of Antennas and Propagation*, vol. 2014, Article ID 593259, 10 pages, 2014.

[15] W. Kang, S. Lee, and K. Kim, "A pattern-reconfigurable antenna using PIN diodes," *Microwave and Optical Technology Letters*, vol. 53, no. 8, pp. 1883–1887, 2011.

[16] Z. Li, E. Ahmed, A. M. Eltawil, and B. A. Cetiner, "A beam-steering reconfigurable antenna for WLAN applications," *IEEE Transactions on Antennas and Propagation*, vol. 63, no. 1, pp. 24–32, 2015.

[17] M. Jusoh, T. Aboufoul, T. Sabapathy, A. Alomainy, and M. R. Kamarudin, "Pattern-reconfigurable microstrip patch antenna with multidirectional beam for WiMAX application," *IEEE Antennas and Wireless Propagation Letters*, vol. 13, pp. 860–863, 2014.

[18] K. Daheshpour, S. Jalali Mazlouman, A. Mahanfar et al., "Pattern reconfigurable antenna based on moving V-shaped

parasitic elements actuated by dielectric elastomer," *Electronics Letters*, vol. 46, no. 13, pp. 886–888, 2010.

[19] J.-J. Liang, G. L. Huang, K. W. Qian, S. L. Zhang, and T. Yuan, "An azimuth-pattern reconfigurable antenna based on water grating reflector," *IEEE Access*, vol. 6, pp. 34804–34811, 2018.

[20] M. S. Alam and A. Abbosh, "Planar pattern reconfigurable antenna with eight switchable beams for WiMax and WLAN applications," *IET Microwaves, Antennas & Propagation*, vol. 10, no. 10, pp. 1030–1035, 2016.

[21] R. Bancroft and B. Bateman, "An omnidirectional planar microstrip antenna," *IEEE Transactions on Antennas and Propagation*, vol. 52, no. 11, pp. 3151–3153, 2004.

[22] J. Li, "An omnidirectional microstrip antenna for WiMAX applications," *IEEE Antennas and Wireless Propagation Letters*, vol. 10, pp. 167–169, 2011.